Two-Dimensional Viscous Simulation of Inlet/Diffuser Flows with Terminal Shocks

Noel A. Talcott Jr.* and Ajay Kumar†
NASA Langley Research Center, Hampton, Virginia

Two-dimensional Navier-Stokes solutions of the flow through three inlet/diffuser configurations with terminal shock systems are reported. Calculations without bleed indicate that the terminal shock location is very sensitive to the outflow back pressure. For cases where there are little or no available experimental results, it becomes difficult to estimate the back pressure that will result in a terminal shock. Estimates based on quasi-one-dimensional analysis are not found adequate for complex two-dimensional flows. It is found that since the flow downstream of the terminal shock is subsonic, and what happens at the outflow boundary affects the flow inside the inlet, enough of the subsonic diffuser must be modeled to accurately predict the terminal shock region. The diffuser portion should be fairly long with the outflow boundary occurring in a region of more or less uniform flow to be able to prescribe a uniform back pressure. The second configuration studied was investigated with and without incorporating bleed in the code. It is found that the use of bleed stabilizes the shock location and allows solutions which, without bleed, result in unstarting of the inlet. The third configuration required a significant amount of bleed through the ramp and cowl surfaces (both ahead and behind the throat) to avoid separation and provide uniform flow at the engine-face station. Comparisons are made with available experimental data.

Nomenclature

h = throat height
M = Mach number
P = pressure, N/m^2
Re = Reynolds number
T = temperature, K
x = streamwise location from the inlet face
α = angle of attack

Subscripts

b = outflow boundary conditions
i = inflow boundary conditions
0 = stagnation
∞ = freestream condition

Introduction

THE design of advanced supersonic aircraft configurations requires accurate estimates of the vehicle's flight characteristics and performance. These estimates must address both the external aircraft aerodynamic characteristics as well as the performance of the proposed propulsion system. The propulsion systems on supersonic aircraft tend to be very large in size and weight, and the integration of the airframe/propulsion system becomes an important consideration to maximize the aerodynamics characteristics of the configuration. An efficient propulsion system would be one whose size and weight have been minimized but whose performance meets the requirements for the aircraft configuration. Linear and nonlinear analysis techniques now provide good estimates of the external aircraft aerodynamic characteristics, and similar analysis tools are needed in the design of the propulsion system. Candidate inlet/diffuser and nozzle designs need to be evaluated for various flight conditions. An important part of this evaluation centers around the nature and location of the terminal shock in the inlet/diffuser. The structure of the shock and its location is critical to the performance and stability of the inlet flow. An efficient inlet design optimizes the terminal shock location to maximize the stability and minimize the losses in the inlet. The flow in the terminal shock region is highly complex. It is primarily turbulent and involves shock/boundary-layer interaction and separation ahead and behind the shock. Further, the location of the shock is highly sensitive to area changes in the diffuser and, therefore, the three-dimensional nature of the flow. New inlet/diffuser concepts have rapidly grown in geometric complexity and do not lend themselves to simple analytic estimates. The alternatives are either to test each concept in the wind tunnel or to numerically calculate the flow with suitable analytic modeling. Experimental testing of each concept is not feasible because of model complexity, cost, and time requirements. A need exists, therefore, to develop a numerical solution technique that can correctly predict the flow in inlets/diffusers, including the terminal shock region. In the present study, a two-dimensional Euler/Navier-Stokes code is used as an initial step toward developing a technique to investigate such flows. Flow calculations are presented with the emphasis of the paper mostly on modeling the viscous flow with a terminal shock system and the investigation of boundary-layer bleed to control and stabilize the terminal shock. Three two-dimensional inlet/diffuser configurations are selected for analysis both with and without bleed. Detailed flowfield results are presented for each configuration, and comparisons are made with available experimental data.

Outline of Method

The present study uses the two-dimensional code described in Refs. 1 and 2 for analyzing flow through inlets/diffusers. The code uses the Euler or Navier-Stokes equations in conservation form as the governing equations. The equations in the physical domain are transformed to the regular computational domain by using an algebraic numerical coordinate transformation that generates a set of boundary-fitted curvilinear coordinates.[3] The transformed equations are solved by an explicit or explicit-implicit method due to MacCormack.[4,5] The

Presented as Paper 84-1362 at the AIAA/ASME/SAE 20th Joint Propulsion Conference, Cincinnati, Ohio, June 11-13, 1984; received Aug. 28, 1984; revision received Dec. 3, 1984.

*Aerospace Engineer, Advanced Concepts Branch, High-Speed Aerodynamics Division. Member AIAA.

†Aerospace Engineer, Computational Methods Branch, High-Speed Aerodynamics Division. Member AIAA.

code can analyze inviscid or viscous (laminar and turbulent) flow. For the case of turbulent flow, an algebraic, two-layer eddy viscosity model due to Baldwin and Lomax[6] is used to estimate the turbulent viscosity. The code is operational on the Control Data VPS-32 vector processing computer system at the Langley Research Center and has been optimized to take maximum advantage of the vector processing capability of the computer.

Boundary and Initial Conditions

No-slip boundary conditions are used on the solid boundaries. For a supersonic inflow boundary, all flow quantities are prescribed whereas, for a subsonic inflow boundary, total pressure and total temperature are prescribed along with the flow angle. For the subsonic inflow case, the pressure at the inflow is extrapolated from the interior points, thus allowing the required upstream influence in the subsonic flow region. All flow quantities are extrapolated for the case of a supersonic outflow boundary. For a subsonic outflow boundary, pressure at the outflow is prescribed and the remainder of the flow quantities are obtained by extrapolation.

Initial flow conditions in the inlet/diffuser are prescribed arbitrarily by using experimentally measured flow quantities, if available, or by assuming freestream conditions at all grid points except at the boundaries where the proper boundary conditions are applied.

Discussion of Results

Several inlet/diffuser models have been analyzed to evaluate the code for simulating flow with a terminal shock. Approximately 3000 grid points were used in each of the calculations with the grid highly refined near the solid boundaries to resolve the viscous effects. Reference 7 presents the inviscid results for the initial supersonic inlet configuration studied. These calculations showed that the terminal shock location was very sensitive to the outflow back pressure. Several values of back pressure were tried before establishing a back-pressure value that would cause a terminal shock. In the absence of experimental results, as was the case for the initial configuration, it may be very difficult and time-consuming to estimate the back pressure that will result in a terminal shock—especially for configurations with complex two- and three-dimensional flows. Estimates based on quasi-one-dimensional analysis did not prove adequate. The calculations for the initial supersonic inlet configuration also demonstrated that since the flow downstream of the terminal shock is subsonic, what happens at the outflow affects the flow inside the inlet. Enough of the subsonic flow must be modeled to accurately predict the terminal shock region. The diffuser portion should be fairly long, with the outflow boundary occurring in a region of more or less uniform flow. These observations led to the selection of the three inlet/diffuser configurations reported herein. Results of the two-dimensional viscous analysis for these configurations are presented and comparisons made with available experimental data.

The first model matches the inlet configuration from a detailed experimental investigation,[8] which includes the terminal shock region. Figure 1 shows a simplified schematic of the experimental model, details of which can be found in Ref. 8. Note the long diffuser portion and constant area outflow section which should result in a fairly uniform flow at the exit. The first calculation is obtained with flow conditions that produce transonic diffuser flow with a normal shock. The inflow conditions correspond to a total pressure of $P_0 = 102170$ N/m^2, a total temperature of $T_0 = 300$ K, and a Mach number of about 0.46, which gives a Reynolds number of $Re = 4.73 \times 10^5$ based on throat height h of 44 mm. The outflow back pressure is held fixed at 82452 N/m^2. Given these conditions at the entrance and exit, the flow accelerates to supersonic Mach numbers and then shocks down to subsonic Mach numbers across a terminal normal shock. Figure 2

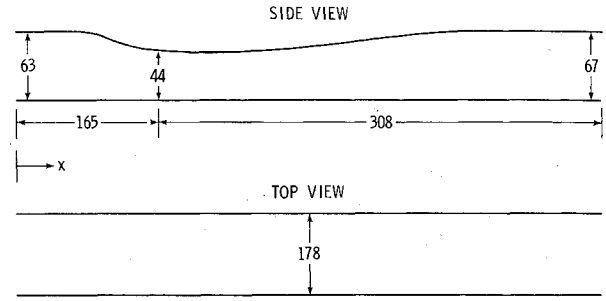

Fig. 1 Simplified schematic of experimental inlet/diffuser model (all dimensions in mm).

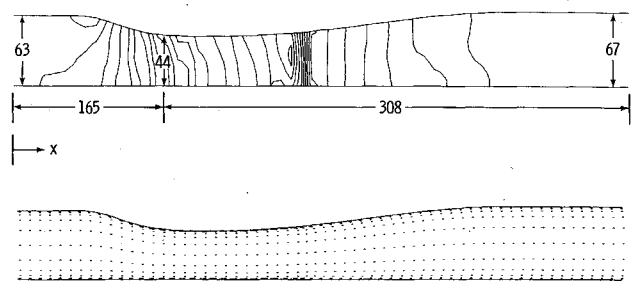

Fig. 2 Pressure contours and velocity vector field in inlet for turbulent flow ($P_b/P_i = 0.933$, $M_i \approx 0.46$).

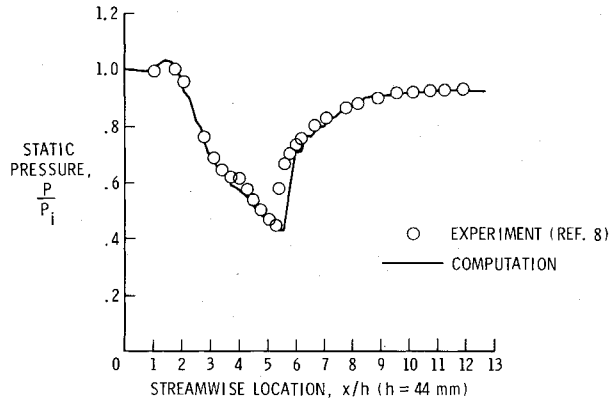

Fig. 3 Pressure distributions on the top surface of the inlet for turbulent flow ($M_i \approx 0.46$).

shows the pressure contours and velocity vector field in the inlet for turbulent flow calculations. The location of the normal shock is clearly seen in the figure. The calculated top and bottom surface pressure distributions are compared with the experimental data of Ref. 8 in Figs. 3 and 4. It is seen that the calculations are in very good agreement with the experimental results. Results for this case have also been obtained by Liu et al. (Refs. 9 and 10) in their numerical study of flows with terminal shocks. The present calculations are also comparable with those calculations. As noted in Ref. 9, the calculations are found to very sensitive to the artificial damping that is added to keep the numerical scheme stable. Too much damping causes the flow to stay subsonic all through the inlet. It is also observed that for this problem, use of the explicit-implicit finite-difference method in the present code is necessary to obtain the solution economically. Use of the fully explicit method requires too many time steps to converge because the flow in this case is predominantly subsonic and the grid used is highly refined near the solid boundaries to resolve the viscous effects.

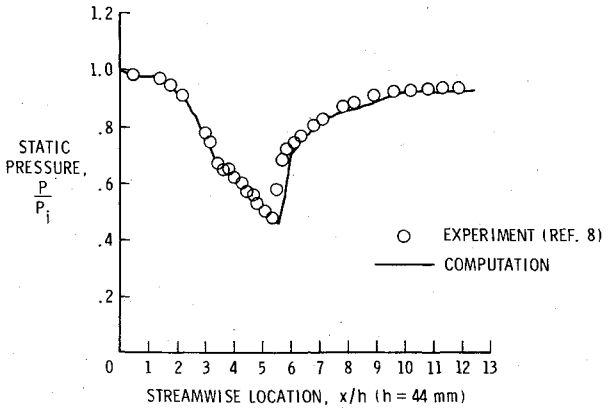

Fig. 4 Pressure distributions on the lower surface of the inlet for turbulent flow ($M_i \approx 0.46$).

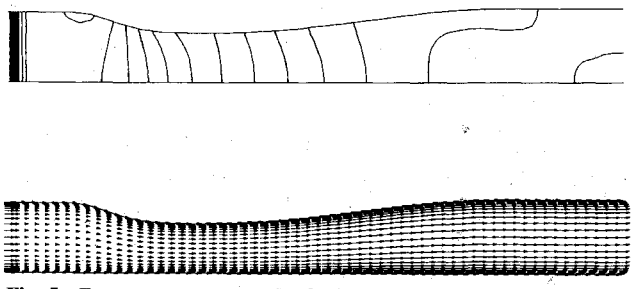

Fig. 5 Pressure contours and velocity vector field in choked inlet for viscous flow ($M_i = 1.90$).

The preceeding configuration is not representative of a supersonic aircraft inlet, and no experimental data are available for supersonic inflow conditions. Liu et al.[9] have presented some results for this configuration with supersonic inflow conditions and a terminal shock system to demonstrate the capability of their numerical code. Calculations were made for an inflow Mach number of 1.9 and the total pressure and temperature from the preceding subsonic inflow case. An attempt was made to repeat this case with the present code. Normally the first step in this type of calculation is to obtain a fully supersonic solution through the duct and then impose the fixed back pressure to force a terminal shock in the diffuser. Given the above inflow conditions, not even a supersonic solution could be obtained for either inviscid or viscous flow. The calculations showed a large increase in pressure just downstream of the inflow boundary and a severe mass imbalance formed. The calculations were terminated at this point, and plots were made for the pressure contours and velocity vector field. These are shown in Fig. 5 for the viscous flow calculations. It is evident from this figure that the inlet is aerodynamically choked. Results similar to those in Fig. 5 are also reported in Ref. 11, where the calculations are made with a fully implicit method. During the course of calculating this case, it was observed that the flowfield at some intermediate time step looked very similar to that reported in Ref. 9, but it is evident that the inlet will not start at $M = 1.9$.

The inflow Mach number was increased to determine the value at which a supersonic solution was possible for the preceding inlet configuration. Inviscid calculations allowed a supersonic flow through the inlet at $M_i = 1.95$, but the inflow Mach number had to be greater than 2.2 to obtain a viscous solution. At this high inflow Mach number, the Mach number in the diffuser is also very high ($M \sim 1.7$) which, given the proper back pressure, will result in a very strong terminal shock. For viscous flow calculations, this will produce a large separation and will undoubtedly require boundary-layer bleed to prevent aerodynamic choking of the inlet.

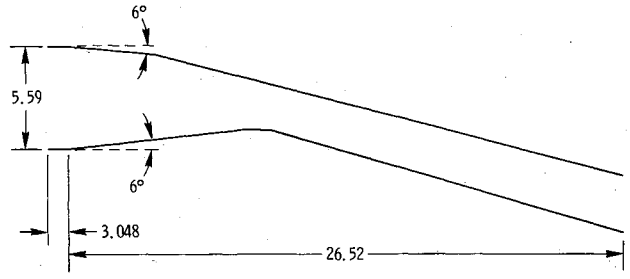

Fig. 6 Sketch of side-mounted integral rocket-ramjet inlet (dimensions in cm).

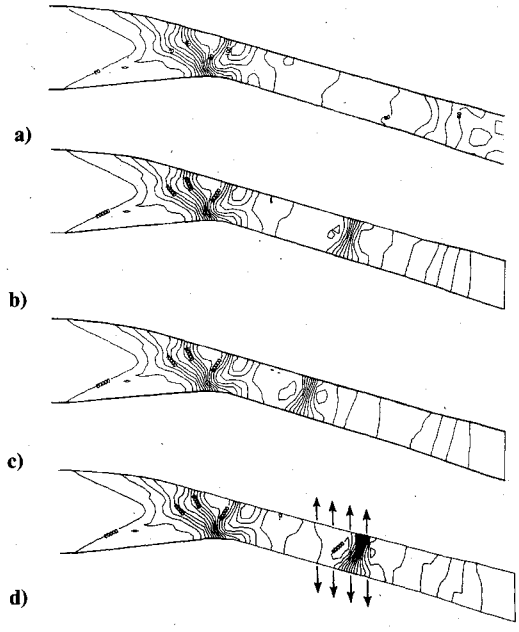

Fig. 7 Pressure contours in side-mounted supersonic inlet ($M_i = 2.5$, $\alpha = 0$): a) fully supersonic flow; b) supersonic inflow, subsonic outflow ($P_b/P_i = 10.32$); c) supersonic inflow, subsonic outflow ($P_b/P_i = 10.88$); d) supersonic inflow, subsonic outflow with bleed ($P_b/P_i = 10.88$, bleed zone indicated by arrows).

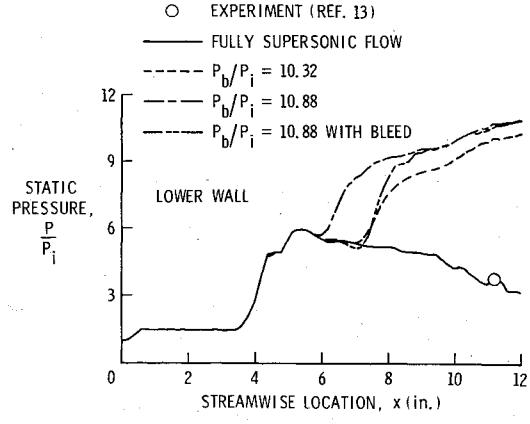

Fig. 8 Pressure distributions on the lower wall of the side-mounted supersonic inlet for turbulent flow ($M_i = 2.5$, $\alpha = 0$).

The second inlet/diffuser configuration to be discussed was selected since it is more representative of an actual supersonic configuration. The configuration is based on the propulsion system of an aft inlet integral rocket-ramjet missile for advanced surface-to-air missions (IRR-SAM).[12] A sketch of the inlet with dimensions is shown in Fig. 6. It was tested side-mounted on a missile forebody. Details of the model and ex-

perimental tests were provided by White and Stevens.[13] Results are presented here for the calculations made at the design Mach number of 2.5 and zero angle of attack. The total pressure and temperature are 287304 N/m^2 and 317 K, respectively. The inflow conditions at the inlet face are obtained by using the method of Ref. 14 to compute the flow over the von Kármán/cylinder forebody. These conditions are $P_i = 16086$ N/m^2, $T_i = 141.39$ K, and $M_i = 2.5$.

With the inflow conditions known, the first step in the analysis of the inlet is to compute a fully supersonic solution through the inlet. This solution is used to initialize the calculations with an imposed back pressure to establish a terminal shock in the diffuser. Figure 7 shows the pressure contours in the inlet for four flow situations. Figure 7a shows the results for the fully supersonic case. The calculations predict an average exit-pressure ratio, P_b/P_i, of approximately 3.8, which is in good agreement with the limited experimental data for this configuration. Several calculations are then made with prescribed back pressures to establish a terminal shock. Figure 7b shows the results for a back-pressure ratio, P_b/P_i, of 10.32. The terminal shock can be clearly seen in the diffuser, positioned about halfway between the throat and exit. When the back-pressure ratio, P_b/P_i, is increased to 10.88, the terminal shock moves upstream in the diffuser as shown in Fig. 7c.

In order to study the effect of bleed on shock location, the preceding back-pressure case is repeated with a small amount of bleed imposed slightly downstream of the terminal shock location. The bleed model used is very straightforward. The amount of bleed mass flow is controlled by imposing constant bleed velocitites along the upper and lower walls in the designated bleed zone. The actual amount of bleed is the sum of the products of the bleed velocity, the wall flow density, and the incremental wall areas. The wall density will vary due to the density jump across the terminal shock; therefore, the bleed model simulates a distributed, variable bleed system along the upper and lower walls. For simplicity, the bleed velocity is aligned with the vertical coordinate system and may or may not be normal to the wall. The magnitude of the imposed fixed bleed velocities are calculated using wall density values obtained from the fully supersonic flow solution. The velocities are selected to bleed a given percentage of the incoming flow through the upper and lower bleed zones. As stated above, the final bleed rates are determined by the converged solution wall densities in the shock/bleed zone.

Results presented in Fig. 7c are repeated with a small amount of bleed located between $x = 6.8$ (17.27 cm) and $x = 8.2$ (20.82 cm). The magnitudes of fixed velocities in the bleed zone are set to 2.3 m/s on the upper wall and 2.6 m/s on the lower wall. These bleed velocities are calculated from the fully supersonic flow solution in Fig. 7a to bleed approximately 1% of the incoming flow equally between the upper and lower wall. Figure 7d shows the effect of bleed on the terminal shock location. It is seen that, in the presence of bleed, the terminal shock moved downstream and positioned itself somewhere in the bleed zone, indicating that bleed can be used to change the terminal shock location to enhance inlet performance. The actual amount of bleed in this case is approximately 3% of the ineoming flow. The larger bleed is due to the density jump across the terminal shock located in the bleed zone.

Figures 8 and 9 show the calculated lower and upper wall surface pressure distributions for the preceding four flow conditions. Movement of the terminal shock due to change in back pressure or introduction of bleed can be clearly seen from these figures. Also, the pressure distributions in the supersonic portion of the flow are unaffected by the presence of the terminal shock.

Bleed is routinely used, and most likely required, to stabilize and position the terminal shock system in actual inlet/diffuser configurations. The preceding results showed how the terminal shock location changed with back pressure and bleed. If the outflow back pressure is increased sufficiently, the inlet will ultimately choke. The next set of calculations show just such a situation and how bleed can be used to stabilize and position the terminal shock in the diffuser.

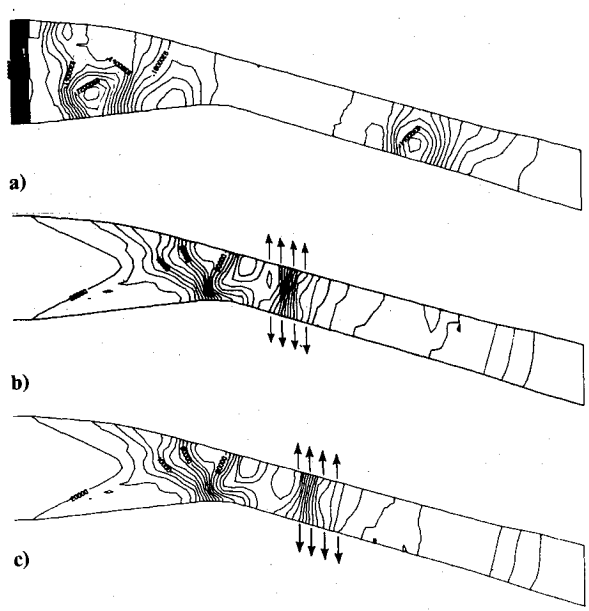

Fig. 10 Pressure contours in side-mounted supersonic inlet with bleed ($M_i = 2.5$, $\alpha = 0$, $P_b/P_i = 11.81$): a) aerodynamically choked—no bleed; b) with bleed; c) bleed zone moved slightly downstream.

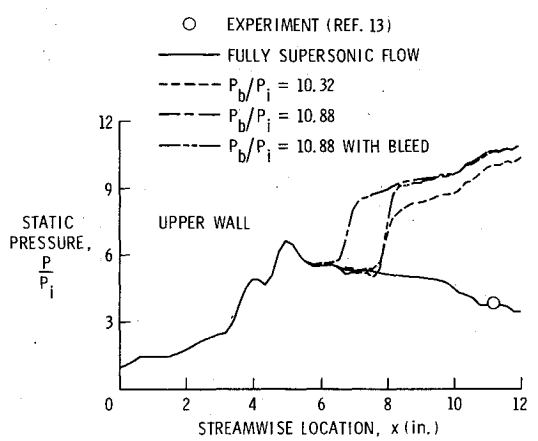

Fig. 9 Pressure distributions on the upper wall of the side-mounted supersonic inlet for turbulent flow ($M_i = 2.5$, $\alpha = 0$).

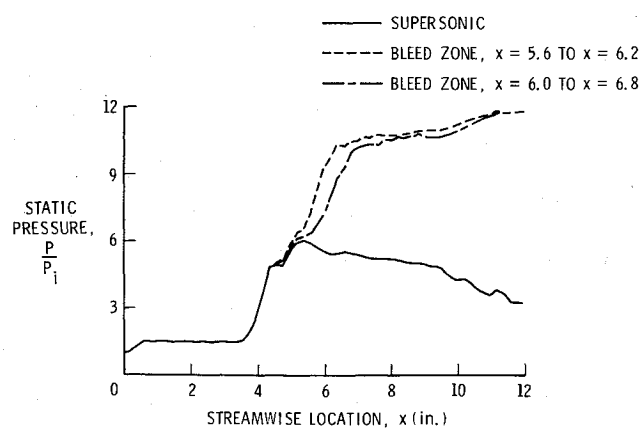

Fig. 11 Pressure distributions on the lower wall of the side-mounted supersonic inlet with bleed ($M_i = 2.5$, $\alpha = 0$, $P_b/P_i = 11.81$).

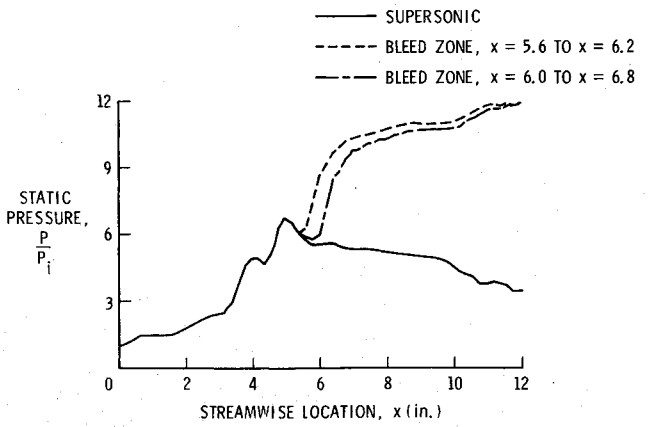

Fig. 12 Pressure distributions on the upper wall of the side-mounted supersonic inlet with bleed ($M_i = 2.5$, $\alpha = 0$, $P_b/P_i = 11.81$).

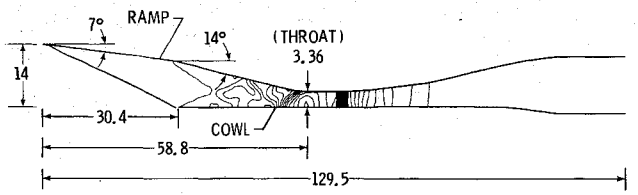

Fig. 13 Pressure contours in two-dimensional supersonic inlet in ($M_\infty = 3.0$, $\alpha = 0$, $P_b/P_\infty \approx 32$); all dimensions in inches.

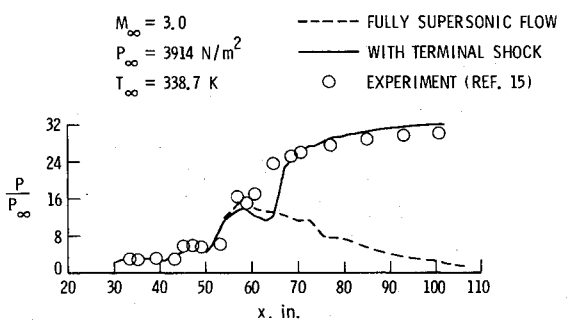

Fig. 14 Pressure distributions on the cowl of the two-dimensional supersonic inlet ($M_\infty = 3.0$, $\alpha = 0$, $P_b/P_\infty \approx 32$).

Figure 10 shows the pressure contours in the inlet for three flow conditions: inlet unstarted, a fixed back pressure with bleed, and the fixed back pressure with the bleed zone moved slightly downstream. The inflow conditions remain unchanged, but the back-pressure ratio, P_b/P_i, is increased to 11.81. With this value of back pressure and no bleed, Fig. 10a shows the inlet in an aerodynamically choked condition. The placement of bleed zones along the upper and lower walls are then used to position the terminal shock in the diffuser slightly downstream of the throat. As with the selection of back pressure, in the absence of experimental data, several calculations were required to determine the appropriate magnitude of the bleed along the walls to prevent large separations and its induced effects. Bleed of approximately 1% of the incoming mass flow through the upper wall and 4% through the lower wall worked well. The bleed zone is located between $x = 5.6$ (14.22 cm) and $x = 6.2$ (15.75 cm), and the magnitudes of the bleed velocities are held constant at 2 m/s through the upper wall and 10 m/s on the lower wall. The pressure contours for the converged bleed solution are shown in Fig. 10b. Figure 10c demonstrates the ability to reposition the terminal shock by moving the bleed zone. In this calculation, parameters remain the same, but the bleed zone is positioned slightly downstream between $x = 6.0$ (15.24 cm) and $x = 6.8$ (17.27 cm). Clearly the

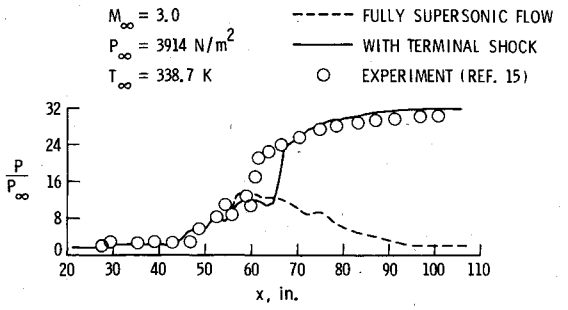

Fig. 15 Pressure distributions on the ramp of the two-dimensional supersonic inlet ($M_\infty = 3.0$, $\alpha = 0$, $P_b/P_\infty \approx 32$).

supersonic portion of the flow remains unchanged, with the net effect being movement of the shock system downstream so that it lies within the new bleed zone.

Figures 11 and 12 show the calculated lower and upper wall surface pressure distributions for three flow conditions: fully supersonic flow and the two cases shown in Figs. 10b and 10c. These figures again show the movement of the shock and its position within the bleed zone. Bleed has been successfully used along the diffuser upper and lower walls to stabilize the terminal shock location and prevent inlet unstart.

The third and final inlet/diffuser system to be discussed wall selected on the basis of its extensive experimental data base. Experimental wall pressure values, as well as bleed location and rates, are available for comparison with the numerical solution. Figure 13 shows a sketch of the configuration with the dimensions given in inches. Details of the model and the experimental data at the design Mach number of 3.0 can be found in Ref. 15. In the experimental test, boundary-layer bleed was used both upstream and downstream of the throat. In addition, vortex generators were used in the diffuser section for forced mixing of the flow to avoid flow separation and to provide more uniform flow at the engine-face station. Results are presented here for the calculations made at the design Mach number of 3.0 and zero angle of attack. The freestream (inflow) pressure and temperature are 3914 N/m^2 and 338.7 K, respectively.

In simulating the preceding flow, a fully supersonic flow solution is obtained through the configuration at the design inflow Mach number of 3.0. A significant amount of bleed is required through the ramp and cowl (both ahead and behind the throat) even to obtain the supersonic solution. The bleed locations and magnitudes are selected to match the experimental values. Several calculations are required to adjust the bleed rates to minimize separation on the ramp and cowl. The supersonic solution is then used to establish a terminal shock in the diffuser by imposing an experimentally measured back pressure of approximately 32 times the freestream pressure. Since the numerical calculations could not simulate the vortex generators employed in the experiment, a slightly higher amount of bleed is used in the calculation to avoid flow separation in the diffuser.

Figure 13 shows the pressure contours in the inlet with the terminal shock clearly evident in the diffuser. The surface pressure distributions on the ramp and cowl are compared with the experimental data in Figs. 14 and 15, respectively. The calculations are in good agreement with the measured levels. The terminal shock is predicted slightly downstream of the measured location. This is due to the additional bleed required in the throat and terminal shock region in the calculations to avoid flow separation in the diffuser in the absence of vortex generators.

The results presented for the three configurations demonstrate the development of a numerical simulation technique for modeling the flow in inlet/diffuser configurations, including the terminal shock region. Calculations are in good agreement with available experimental data including

the location of the terminal shock. The bleed model used in the calculations performed well for the third inlet configuration. The terminal shock location was predicted slightly downsteam of the measured location due to additional bleed requirements necessary to avoid flow separation in the diffuser in the absence of vortex generators.

Concluding Remarks

Two-dimensional Navier-Stokes solutions for the flow through three inlet/diffuser configurations with terminal shocks have been obtained. It is observed that the use of the explicit-implicit finite-difference method is necessary to obtain the solution economically. The fully explicit method requires too many time steps to converge due to the large regions of subsonic flow and the highly refined grid used near the solid boundaries to resolve the viscous effects. Calculations without bleed indicate that the terminal shock location is very sensitive to outflow back pressure and that choking of the inlet is inevitable as the magnitude of the back pressure increases. Bleed along the diffuser upper and lower walls can be used to stabilize the terminal shock location and prevent choking of the inlet. The absence of detailed experimental data makes it difficult to: 1) estimate the back pressure that will force a terminal shock in the diffuser and 2) determine the magnitude of bleed required to stabilize and position the shock. It is also observed that in order to be able to prescribe a uniform back pressure at the outflow boundary to establish a terminal shock, the diffuser section should be fairly long, with the outflow boundary occurring in a region of more or less uniform flow.

Comparisons with available experimental data are in good agreement, including the location of the terminal shock. The bleed model used in the calculations worked well for the third configuration examined, which experimentally employed several bleed zones and extensive amounts of bleed. The terminal shock location was predicted downstream of the experimentally measured location due to additional bleed required in the throat and terminal shock region to avoid flow separation in the diffuser in the absence of vortex generators.

Work continues on validation of the analysis prior to moving to three-dimensional calculations. Three-dimensional analysis capability will surely be required to resolve the three-dimensional nature of the flow in configurations incorporating area changes in the diffuser (transition from rectangular to nonrectangular cross sections) or the multizone, multiwall bleeds common in today's advanced inlet concepts.

References

[1]Kumar, A., "Numerical Analysis of the Scramjet-Inlet Flow Field by Using Two-Dimensional Navier-Stokes Equations," NASA TP-1940, Dec. 1981.

[2]Kumar, A. "User's Guide for NASCRIN—A Vectorized Code for Calculating Two – Dimensional Supersonic Internal Flow Fields," NASA TM-85708, Feb. 1984.

[3]Smith, R.E., "Two-Boundary Grid Generation for the Solution of the Three-Dimensional Compressible Navier-Stokes Equations," NASA TM-83123, May 1981.

[4]MacCormack, R.W., "The Effect of Viscosity in Hypervelocity Impact Cratering," AIAA Paper 69-354, May 1969.

[5]MacCormack, R.W., "A Numerical Method for Solving the Equations of Compressible Viscous Flow," AIAA Paper 81-0110, Jan. 1981.

[6]Baldwin, B.S. and Lomax, H., "Thin-Layer Approximation and Algebraic Model for Separated Turbulent Flows," AIAA Paper 78-257, Jan. 1978.

[7]Talcott, N.A. Jr. and Kumar, A., "Numerical Simulation of Flow Through Inlets/Diffusers with Terminal Shocks," AIAA Paper 84-1362, June 1984.

[8]Boger, T.J., Sajben M., and Kroutil, J.C., "Characteristic Frequency and Length Scales in Transonic Diffuser Flow Oscillations." AIAA Paper 81-1291, June 1981.

[9]Liu, N.-S., Shamroth, S.J., and McDonald, H., "Numerical Solution of the Navier-Stokes Equations for Compressible Turbulent Two/Three Dimensional Flows in the Terminal Shock Region of an Inlet/Diffuser," AIAA Paper 82-1892, July 1983.

[10]Liu, N.-S., Shamroth, S.J., and McDonald, H., "Numerical Solutions of the Navier-Stokes Equations for Compressible Turbulent Two/Three Dimensional Flows in the Terminal Shock Region of an Inlet/Diffuser," Final Report for NAS-22747, Nov. 1982.

[11]Walters, R.W., "LU Methods for the Compressible Navier-Stokes Equations," Ph.D. Dissertation, North Carolina State University, Raleigh, N.C., March 1984.

[12]Aeronautics Division, "Preliminary Evaluation of Propulsion System of an Aft Inlet Integral Rocket-Ramjet Missile for Advanced Surface-to-Air Missions, IRR – SAM," Applied Physics Laboratory, Johns Hopkins University, Baltimore, Md., TM TG-693, May 1965.

[13]White, M.E. and Stevens, J.R., Private Communication, Applied Physics Laboratory, Laurel, Md. Jan. 1984.

[14]Salas, M.D., "Shock Fitting Method for Complicated Two-Dimensional Supersonic Flows," *AIAA Journal*, Vol. 14, No. 5., May 1976, pp. 583-588.

[15]Anderson, E. and Wong, N.D., "Experimental Investigation of a Large-Scale, Two-Dimensional, Mixed Compression Inlet System—Performance at Design Conditions, $M_\infty = 3.0$," NASA TM X-2016, May 1970.